JOURNAL OF VIROLOGY, July 2004, p. 6808–6817 Vol. 78, No. 13
0022-538X/04/$08.00+0 DOI: 10.1128/JVI.78.13.6808–6817.2004
Copyright © 2004, American Society for Microbiology. All Rights Reserved.

Transduction Profiles of Recombinant Adeno-Associated Virus Vectors Derived from Serotypes 2 and 5 in the Nigrostriatal System of Rats

Jean-Charles Paterna,[1]* Joram Feldon,[2] and Hansruedi Büeler[1]

Institute of Molecular Biology, University of Zurich, 8057 Zurich,[1] and Laboratory of Behavioural Neurobiology, ETH Zurich, 8603 Schwerzenbach,[2] Switzerland

Received 10 October 2003/Accepted 1 March 2004

We compared the transduction efficiencies and tropisms of titer-matched recombinant adeno-associated viruses (rAAV) derived from serotypes 2 and 5 (rAAV-2 and rAAV-5, respectively) within the rat nigrostriatal system. The two serotypes (expressing enhanced green fluorescent protein [EGFP]) were delivered by stereotaxic surgery into the same animals but different hemispheres of the striatum (STR), the substantia nigra (SN), or the medial forebrain bundle (MFB). While both serotypes transduced neurons effectively within the STR, rAAV-5 resulted in a much larger EGFP-expressing area than did rAAV-2. However, neurons transduced with rAAV-2 vectors expressed higher levels of EGFP. Consistent with this result, EGFP-positive projections emanating from transduced striatal neurons covered a larger area of the SN pars reticulata (SNr) after striatal delivery of rAAV-5, but EGFP levels in fibers of the SNr were higher after striatal injection of rAAV-2. We also compared the potentials of the two vectors for retrograde transduction and found that striatal delivery of rAAV-5 resulted in significantly more transduced dopaminergic cell bodies within the SN pars compacta and ventral tegmental area. Similarly, EGFP-transduced striatal neurons were detected only after nigral delivery of rAAV-5. Furthermore, we demonstrate that after striatal AAV-5 vector delivery, the transduction profiles were stable for as long as 9 months. Finally, although we did not target the hippocampus directly, efficient and widespread transduction of hippocampal neurons was observed after delivery of rAAV-5, but not rAAV-2, into the MFB.

With the exception of rare inherited mutations in specific genes that segregate with familial forms of Parkinson's disease (PD) (24, 29, 30, 42), the molecular causes of PD remain unknown. Pathologically, PD is caused by the progressive degeneration of the dopaminergic neurons in the substantia nigra pars compacta (SNc), which is accompanied by a corresponding decline of the neurotransmitter dopamine in the striatum (STR). As a consequence, PD patients present with resting tremor, bradykinesia, rigidity, and postural instability. Dopamine replacement therapy using L-dopa is the most frequent treatment for PD, but its beneficial effects wear off over time and severe side effects often occur. Surgical treatments such as pallidotomy, thalamotomy, or deep brain stimulation as well as cell transplantation therapies ameliorate some of the symptoms but do not inhibit ongoing neurodegeneration. With increasing knowledge about molecular mechanisms of neuron death (19), gene therapy may offer the potential to interfere with the pathophysiological mechanisms causing cell death in PD. Previous gene therapy studies in rodent and nonhuman primate models of PD assessed the protective potential of neurotrophic, antiapoptotic, antioxidative, and dopamine-restorative genes delivered by recombinant adenovirus (rAV) (8), lentivirus (28), herpes simplex virus (13), adeno-associated virus (rAAV) (22), or hybrid viral (9) vectors. Besides the choice of the viral vector and the gene delivered, an important aspect for the success of these studies has been the design of transgene cassettes optimized for sustained and high-level gene expression in the brain (39).

rAAV vectors have gained much attention due to their ability to mediate efficient transduction of dividing and nondividing cells and to support long-term gene expression in the absence of toxicity. Over the last decade, rAAV vectors derived predominantly from serotype 2 (rAAV-2) were generated and investigated in vivo. The recent discovery of human and nonhuman AAVs distinct from serotype 2 (serotypes 1 and 3 to 8) and the cloning of their genomes have enabled scientists to generate pseudotyped rAAV vectors and to increase the potency of rAAV-2 vector-based gene therapy approaches (6, 7, 16, 45, 52). Notably, the newly identified serotypes were able to extend the tropism and to exceed the in vivo transduction efficiency of rAAV-2 vectors by several orders of magnitude in organs such as the lung (53) and the liver (18) and in skeletal muscles (5). Until now, only a limited number of gene transfer studies within the central nervous system have been carried out with non-serotype-2 rAAV vectors. Transduction patterns distinct from those of rAAV-2 vectors were observed in the rodent brain after intraventricular (rAAV-1, -4, and -5) (11, 38), striatal (rAAV-1, -4, and -5) (10, 11, 32, 51), cerebellar (rAAV-5) (1), and hippocampal (rAAV-5) (26, 35, 37) delivery. However, no data regarding the transduction profile of rAAV-5 vectors within the entire nigrostriatal system were reported. Therefore, we set out to compare titer-matched rAAV-2 and rAAV-5 vectors in the same animals for their

* Corresponding author. Mailing address: Institute of Molecular Biology, University of Zurich, Winterthurerstrasse 190, 8057 Zurich, Switzerland. Phone: 41-1-635-3180. Fax: 41-1-635-6811. E-mail: smart@molbio.unizh.ch.

abilities to transduce the rat nigrostriatal system. Viruses were delivered into the substantia nigra (SN), the STR, or the medial forebrain bundle (MFB) (the fiber bundle emanating from the SN and projecting into the STR). In each case, expression of enhanced green fluorescent protein (EGFP) was investigated locally in cell bodies at the site of injection, in fibers of transduced neurons (anterograde transport of gene product) projecting to other brain areas, and in neuronal cell bodies that send axons to distantly transduced neurons (retrograde transduction).

MATERIALS AND METHODS

Plasmid constructions. The rAAV-2 vector pAAV-2-CBA-WPRE was constructed by insertion of the Klenow polymerase-filled, 1,723-bp EcoRI CBA promoter fragment derived from plasmid pCBA-GFP-WPRE (25) between the Klenow fragment-filled EcoRI and NheI sites of psub-CMV-WPRE (40). Subsequently, the HpaI/SmaI EGFP fragment from pEGFP-N1 (Clontech, Palo Alto, Calif.) was inserted into the PmlI site of pAAV-2-CBA-WPRE to generate pAAV-2-CBA-EGFP-WPRE. To construct the rAAV-5 vector pAAV-5-CBA-EGFP-WPRE, the entire CMV-EGFP-WPRE expression cassette of plasmid pAAV5.1-EGFP (3) (from James Wilson) was removed by NheI and SphI digestion. Subsequently, the blunted KpnI/SphI CBA-EGFP-WPRE expression cassette (lacking AAV-2 inverted terminal repeats [ITRs]) from pAAV-2-CBA-EGFP-WPRE was ligated between the blunted NheI and SphI sites of pAAV5.1-EGFP such that the CBA-EGFP-WPRE expression cassette was flanked by the AAV-5 ITRs of pAAV5.1-EGFP.

Production, purification, and titration of AAV vector. rAAV-2 vectors were produced by the calcium phosphate precipitation method. Approximately $1.2 \cdot 10^8$ 293T cells (containing the AV genomic regions E1A and E1B) were cotransfected with the rAAV-2 vector plasmid pAAV-2-CBA-EGFP-WPRE and the hybrid AV/AAV helper plasmid pDG (17) (from Juergen Kleinschmidt) at a molar ratio of 1:1. pDG provides in *trans* the helper functions of the AV-5 genomic regions VA, E2A, and E4, as well as the replication and encapsidation functions of the AAV-2 *rep* and *cap* genes, but the endogenous AAV-2 p5 promoter has been replaced by the mouse mammary tumor virus long terminal repeat promoter.

To produce rAAV-5 particles, 293T cells were cotransfected with the rAAV-5 vector pAAV-5-CBA-EGFP-WPRE, the AAV-5 packaging plasmid pack5.1 (3), and the AV helper plasmid pAdΔF6 (54) (the latter two from James Wilson). pack5.1 provides in *trans* the packaging and encapsidation functions of the AAV-5 *rep* and *cap* genes, and pAdΔF6 provides in *trans* the necessary AV helper functions as described for pDG.

Cells were collected by centrifugation 48 to 72 h after transfection, resuspended in 150 mM NaCl–50 mM Tris-HCl (pH 8.5), and lysed by three cycles of freeze-thawing. After a 30-min incubation at 37°C with 50 U of benzonase/ml, the lysates were cleared by centrifugation and purified by iodixanol gradient ultracentrifugation as described elsewhere (55). rAAV-2 vectors were further purified by heparin affinity chromatography as described elsewhere (55). Peak virus fractions were pooled, dialyzed three times for 2 h at room temperature against phosphate-buffered saline (PBS)–1 mM $MgCl_2$, and sterile-filtered by using Millex GV_4 filter units (Millipore, Bedford, Mass.). rAAV-5 vectors were concentrated by centrifugation through Centricon Plus 20 columns (Biomax100 membrane; Millipore) that had been preincubated overnight at 4°C with PBS–1 mM $MgCl_2$–2.5 mM KCl–2% (vol/vol) rat serum. The columns were rinsed twice with PBS–1 mM $MgCl_2$–2.5 mM KCl before the virus-containing iodixanol fraction was applied. Physical titers (in vector genomes [vg] per milliliter) of purified vector stocks were determined by slot blot hybridization using a [^{32}P]dCTP-labeled EGFP probe fragment, and signals were quantified in the PhosphorImager by using ImageQuant software (Molecular Dynamics, Sunnyvale, Calif.).

Animals and surgery. Eight-week-old male Sprague-Dawley rats (291 ± 18 g) were anesthesized by intraperitoneal injection of pentobarbital sodium (Nembutal; 50 mg/kg of body weight) (Abbott Laboratories, North Chicago, Ill.) and placed in a stereotactic frame (Kopf Instruments, Tujunga, Calif.). rAAV-2 and rAAV-5 vectors encoding EGFP were adjusted to $8 \cdot 10^{11}$ vg/ml and injected into separate hemispheres of the same animal. Each brain site (STR, SN, MFB) and hemisphere was injected at two positions with 2 μl of rAAV at a speed of 0.5 μl/min at symmetrical coordinates through a 26-gauge cannula by using a sp2001 precision pump (World Precision Instruments, Sarasota, Fla.). For the short-term expression study (28 days), injections were done at the following stereotaxic coordinates (41): for the SN, −5.3 mm (anterior-posterior [AP]), ±1.8 mm/±2.5 mm (medial-lateral [ML]), and −7.7 mm/−7.3 mm (dorsal-ventral [DV]) (six animals for each vector serotype); for the MFB, −2.8 mm/−3.3 mm (AP), ±1.5 mm (ML), and −8.5 mm (DV) (six animals for each vector serotype); for the STR, ±0.5 mm (AP), ±2.1 mm/±2.9 mm (ML), and −6.5 mm (DV) (six animals for each vector serotype). For the long-term expression study (9 months), two Sprague-Dawley rats (340 and 370 g) each received an injection of 5 μl of rAAV-5 ($2 \cdot 10^{11}$ vg/ml) at two of the following stereotaxic coordinates in the STR of the right hemisphere: AP, ±0.5 mm; ML, +2.5 mm/+3.3 mm; DV, −5.0 mm. Seven Sprague-Dawley rats (342 ± 54 g) each received injections of 1 μl of colchicine solution (20 mg/ml, dissolved in double-distilled H_2O; Sigma, Buchs, Switzerland) at two locations in the MFB of the left hemisphere at the same stereotaxic coordinates as those described for the rAAV-5 injections. Fifteen minutes later, the colchicine injections were followed by rAAV-5. One rat received colchicine only in order to assess the effect of the drug on the integrity of the nigrostriatal pathway. Colchicine and rAAV-5 were delivered by using independent sets of cannulae and tubings.

Histology and microscopy. Animals were anesthesized and decapitated 28 days or 9 months after rAAV injection. Brains were removed, incubated for 2 days at 4°C in 4% paraformaldehyde–PBS, and dehydrated for at least 2 days at 4°C in 30% sucrose–PBS. Consecutive 20-μm-thick coronal cryosections between AP +1.8 mm and −6.3 mm (relative to bregma) were prepared. Sections were incubated for 5 min in 3% H_2O_2–10% methanol–PBS to quench endogeneous peroxidase activity and were blocked for 1 h at room temperature in 0.3% Triton X-100–5% horse serum–0.2% bovine serum albumin–Tris-buffered saline. Sections were incubated overnight at 4°C with the primary antibody in 0.15% Triton X-100–2% horse serum–0.2% bovine serum albumin–Tris-buffered saline, washed, and incubated for 1 to 2 h in the same buffer with a Cy3-conjugated secondary antibody. The following antibodies and dilutions were used: polyclonal sheep anti-tyrosine hydroxylase (anti-TH) (dilution, 1:1,000; Pel-Freez Biologicals, Rogers, Ark.), monoclonal mouse anti-glial fibrillary acidic protein (anti-GFAP; dilution, 1:1,000; PharMingen, San Diego, Calif.), monoclonal mouse anti-glutamic acid decarboxylase (anti-GAD; dilution, 1:1,000; used in the short-term expression study; Chemicon, Temecula, Calif.), polyclonal rabbit anti-GAD65 (dilution, 1:1,000; used in the long-term expression study; Chemicon), monoclonal mouse anti-neuronal nuclei (anti-NeuN; dilution, 1:600; Chemicon), a Cy3-conjugated donkey anti-sheep antibody (dilution, 1:1,200; Milan Analytica, La Roche, Switzerland), and a Cy3-conjugated donkey anti-rabbit antibody (dilution, 1:1,200; Milan Analytica). Fluorochromes were detected by using a microscope (Leica, Mannheim, Germany) equipped with a mercury high-pressure light device and appropriate filters. Sets of images were captured under identical conditions with an AxioCam color charge-coupled device camera and AxioVision 3.0 software (both from Carl Zeiss, Feldbach, Switzerland). Photoshop 6.0 software (Adobe, San Jose, Calif.) was used to process sets of images under identical conditions.

Statistical analysis. Statistical analysis was performed using the Mann-Whitney U test. A U value of ≤ 0.01 was considered significant. Results are presented as the mean ± 1 standard deviation.

RESULTS

Transduction of the nigrostriatal pathway after vector delivery into the STR. (i) STR. Both rAAV serotypes mediated efficient EGFP expression in the injected STR (Fig. 1). Confocal microscopy revealed that the majority of cells transduced within the STR by both serotypes were NeuN-positive cells (insets in Fig. 1C and H). GFAP levels were unaltered with both serotypes relative to those in animals injected with buffer only (data not shown). Sections selected in the rostral part of the STR (around the bregma + 1.6 mm) in five different animals showed weak (Fig. 1B) to intense (Fig. 1A and C to E), but always localized, EGFP expression after rAAV-2 delivery. In contrast, the contralateral rAAV-5-injected STR contained EGFP-positive cells distributed over a much larger area (Fig. 1F to J). Neither of the two serotypes transduced NeuN-positive cell bodies in the more caudal part (around the bregma − 2.3 mm) of the caudate putamen (Fig. 1K to T). However, in the same sections, both serotypes transduced cells located within the globus pallidus (GP) and produced a network of

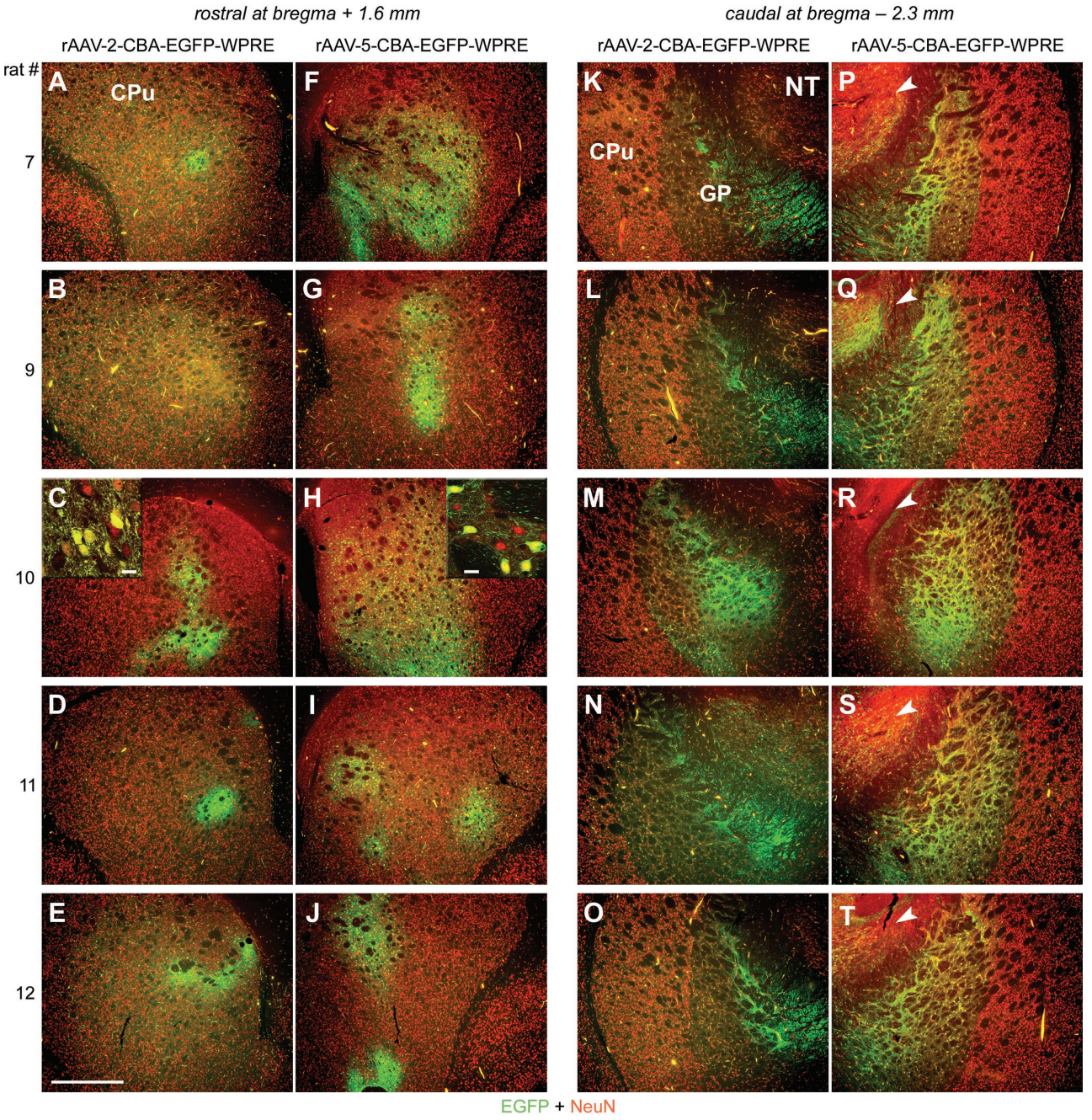

FIG. 1. EGFP expression in the STR after striatal injection of rAAV-2 and rAAV-5. Coronal sections of the STR were analyzed for expression of EGFP (green) and NeuN (red) 28 days after virus injections. Representative two-color (merged) images from five animals are shown. (A to E) Within the rostral part of the STR, rAAV-2-mediated EGFP expression was locally restricted around the needle tract. CPu, caudate putamen. (F to J) In contrast, rAAV-5-mediated EGFP expression was widespread. (C and H insets) Confocal microscopy revealed that the majority of cells transduced within the STR by both serotypes were NeuN positive. Bars for insets, 25 μm. (K to T) Within the caudal part of the STR, EGFP expression was restricted to fibers (both serotypes) and a few positive cells (rAAV-2 [K to O]) in the GP. rAAV-5 transduced more cells within and outside of the GP (e.g., nucleus thalamus [NT; arrowheads in panels P to T]). Bar for panels, 500 μm.

strongly EGFP-positive fibers, indicative of anterograde transport of EGFP within transduced striatal neurons projecting to the SN (Fig. 1K to T). While only a few NeuN and EGFP double-positive cell bodies were detected within the GP after rAAV-2 injections (Fig. 1K to O), significantly more cells were found in the rAAV-5-injected hemisphere (Fig. 1P to T). Furthermore, only rAAV-5 vectors transduced NeuN-positive cell bodies located outside the nigrostriatal pathway (e.g., nucleus thalamicus [Fig. 1P to T]).

(ii) SN. The relationship between the striatal afferents and the lamellar organization of the rat SN pars reticulata (SNr) (12) is reflected by the EGFP expression pattern depicted in

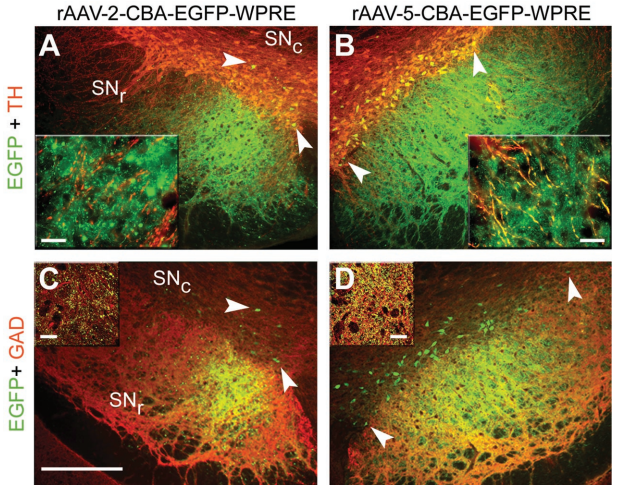

FIG. 2. EGFP expression in the SN after striatal injection of rAAV-2 and rAAV-5. Coronal sections of the SN were analyzed for expression of EGFP (green), TH (red), and GAD (red). Representative two-color (merged) images from one animal are shown. GAD-positive EGFP-expressing fibers emerging from rAAV-5-transduced striatal neurons were detected throughout the SNr (B and D). Fewer EGFP-expressing fibers, located mainly in the medial part of the SNr, were observed after striatal injection of rAAV-2 (A and C). These observations are in accordance with the lamellar organization of the SNr (12). Many dopaminergic (TH-positive) neurons in the SNc expressed EGFP after striatal rAAV-5 injection (B and D, arrowheads), whereas only a few such cells were found after striatal rAAV-2 delivery (A and C, arrowheads). Bar for panels, 250 μm. Bars for insets, 25 μm.

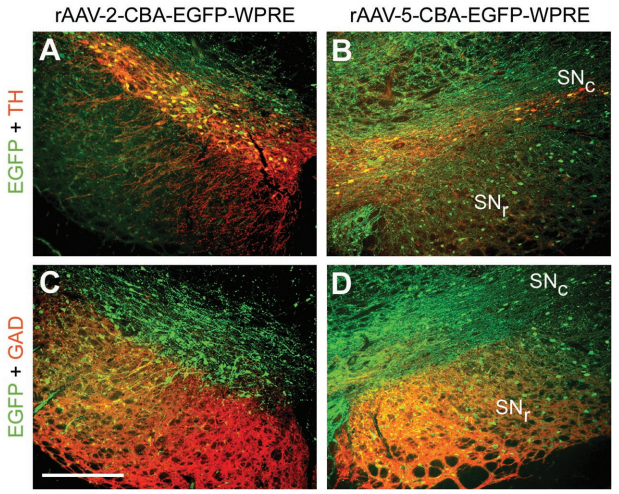

FIG. 3. EGFP expression in the SN after nigral injection of rAAV-2 and rAAV-5. Coronal sections of the SN were analyzed for expression of EGFP (green), TH (red), and GAD (red). Representative two-color (merged) images from one animal are shown. EGFP-expressing TH-positive neurons in the SNc were found for both vector serotypes (A and B). However, significantly more EGFP-positive cells were present in the GAD-positive area of the SNr after nigral rAAV-5 delivery (C and D). Bar, 250 μm.

Fig. 2. GAD-positive projections emanating from striatal neurons projecting into the SNr were found to be EGFP positive after delivery of both vector serotypes into the STR (Fig. 2C and D). However, major differences were observed between the two serotypes. EGFP expression in the SNr after striatal delivery of rAAV-2 vectors was spatially more restricted but reached higher levels in individual fibers (as seen by strongly fluorescent cross-sectioned fibers) than was observed with rAAV-5 (insets in Fig. 2A and B), which resulted in EGFP expression in fibers throughout the SNr (Fig. 2B). Confocal microscopy confirmed this finding and clearly demonstrated a higher number and density of EGFP-positive fibers in the SNr after striatal delivery of rAAV-5 (insets in Fig. 2C and D). The higher density and larger area of EGFP-positive fibers in the SNr is in accordance with the higher number of transduced cells observed after striatal rAAV-5 injection (Fig. 1). Furthermore, retrogradely transduced TH-positive cell bodies located within the SNc were more numerous and were distributed over a larger ML extension after striatal rAAV-5 delivery (Fig. 2B and D) than after striatal rAAV-2 delivery (Fig. 2A and C). Quantification of EGFP-positive cell bodies within the ventral tegmental area (VTA) and the SNc in both hemispheres revealed a significantly higher number of retrogradely transduced neurons for serotype 5 (40.7 ± 13.1 versus 16.6 ± 8.1; $P < 0.001$; four consecutive sections per animal around the bregma [5.3 mm]; five animals)).

Transduction of the nigrostriatal pathway after vector delivery into the SN. (i) SN. Both rAAV serotypes efficiently transduced TH-positive neurons in the SNc (Fig. 3A and B). Again, for both vector serotypes, GFAP levels were not elevated above those in animals injected with buffer only (data not shown). rAAV-2-mediated EGFP expression was mainly confined to the SNc and nearby areas located dorsal to it (Fig. 3A and C). In contrast, rAAV-5 transduced a large area in the entire midbrain (data not shown), including numerous cells within the SNr, an area that was poorly transduced by rAAV-2 (Fig. 3C and D). Quantification of EGFP-positive cell bodies located in the ventral half of the SNr showed that the rAAV-5 vector transduced significantly more cells than the rAAV-2 vector (71.6 ± 24.8 versus 17.3 ± 14.0; $P < 0.001$; three consecutive sections per animal around the bregma [5.3 mm]; six animals).

(ii) STR. Despite efficient expression of EGFP in nigral dopaminergic neurons, EGFP could not be detected in TH-positive axon terminals in the STR for either serotype by native fluorescence microscopy (Fig. 4). However, widespread and strong EGFP expression was detected in fibers of the external capsule (Fig. 4A) and of the capsula interna (CI) (Fig. 4B) after nigral injection of rAAV-5. Moreover, no EGFP-positive neurons in the STR were detected after nigral delivery of rAAV-2, but we found such cells after nigral delivery of rAAV-5 (Fig. 4C) at a frequency of 42.6 ± 26.5 per section (3 consecutive sections per animal around the bregma + 0.2 mm; 6 animals). NeuN staining classified these cells as neurons (Fig. 4D), and their morphology suggested that they were medium-sized spiny projection neurons.

Transduction of the nigrostriatal pathway after vector delivery into the MFB. (i) MFB. EGFP-positive fibers and cell bodies were readily detected within the TH-positive area of the MFB after injection of either rAAV serotype (Fig. 5). Again, as observed in the STR and the SN, rAAV-5 transduced a larger area in the MFB than did rAAV-2 (Fig. 5A and B), with EGFP-positive cell bodies found in the ventral part of the MFB (Fig. 5B).

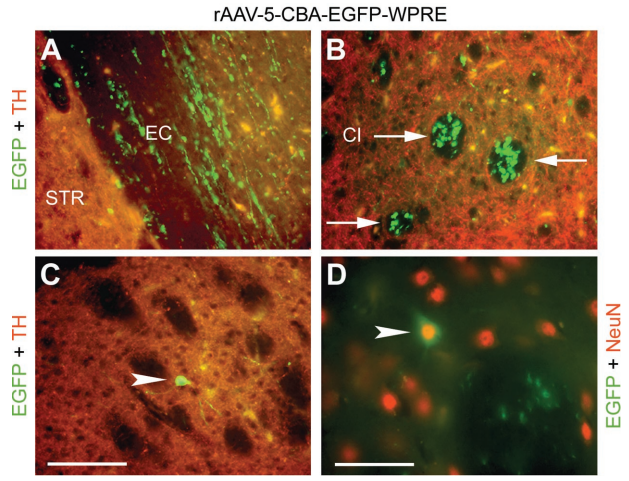

FIG. 4. EGFP expression in the STR after nigral injection of rAAV-2 and rAAV-5. Coronal sections of the STR were analyzed for expression of EGFP (green), TH (red), and NeuN (red). Representative two-color (merged) images of the rAAV-5-injected hemisphere from one animal are shown. Neither EGFP-positive fibers nor EGFP-positive cells were detected after nigral delivery of rAAV-2 (data not shown). In contrast, nigral injection of rAAV-5 resulted in EGFP-positive fibers located within the CI (B, arrows), the external capsule (EC) (A), and the cortex (data not shown). However, neither vector serotype resulted in (detectable) expression of EGFP in TH-positive striatal axons. Retrogradely transduced striatal neurons (C, arrowhead) were detected after nigral injection of rAAV-5 at a frequency of 42.6 ± 26.5 cells per section (3 sections per animal; 6 animals). These EGFP-expressing cells stained positive for NeuN (D, arrowhead), and their morphology suggested that they are medium-sized spiny projection neurons. Bar for panels A to C, 62.5 μm. Bar for panel D, 39.7 μm.

(ii) STR. EGFP-positive fibers were detected in the CI and were present in both hemispheres (Fig. 5C and D), a situation similar to that after nigral rAAV-5 vector delivery (compare Fig. 4B with Fig. 5C and D). In agreement with the stronger EGFP expression in individual fibers of the SNr after striatal rAAV-2 delivery (Fig. 2A), injection of rAAV-2 into the MFB resulted in a stronger EGFP signal within the fibers of the CI than that with injection of rAAV-5 (Fig. 5C and D).

(iii) SN. Delivery of rAAV-2 into the MFB resulted in only a few EGFP-positive fibers located dorsally to the SN (Fig. 5E), and occasionally EGFP-positive cell bodies were found within the SNc (Fig. 5E). However, EGFP-positive fibers surrounding TH-positive dopaminergic neurons after MFB delivery of rAAV-2 vectors could be detected (Fig. 5E). In contrast, rAAV-5 delivery to the MFB resulted in more TH and EGFP double-positive dopaminergic neurons in the SNc (Fig. 5F). In order to distinguish between simple diffusion of rAAV-5 vectors from the MFB to the SNc and retrograde axonal transport, colchicine was injected into the MFB prior to rAAV-5 vector delivery. Colchicine blocks fast axonal transport by interfering with microtubule organization (14), and it has been used to inhibit retrograde transport of rAV and rAAV from the sciatic nerve to the spinal cord in mice and rats (4). In agreement with previous observations (15), the dose of colchicine applied in this study did not change the morphology of TH-positive neurons in the SNc (Fig. 5G), although a reduced striatal TH signal was observed on the colchicine-injected hemisphere (data not shown). However, colchicine blocked rAAV-5-mediated EGFP expression in TH-positive neurons of the SNc and VTA almost completely after virus delivery to the MFB (Fig. 5G).

(iv) Hippocampus. Surprisingly, we found that the hippocampus was efficiently transduced in several animals after MFB injection of rAAV-5 (Fig. 6B and C). Mossy fibers emanating from EGFP-expressing granule cells of the dentate gyrus (DG) were readily identified in the CA3 region (Fig. 6B). Likewise, many NeuN-positive pyramidal cells in the hilus of the DG expressed EGFP (Fig. 6B and C). EGFP-positive fibers derived from transduced pyramidal cells were found in the molecular layer of the hippocampus (Fig. 6B). In addition, some NeuN-negative cells within the DG also expressed EGFP, indicating the transduction of nonneuronal cells by rAAV-5. In contrast, rAAV-2 only weakly transduced hippocampal neurons that were located close to the needle tract (Fig. 6A). Interestingly, as seen for the SNc and VTA (Fig. 5G), colchicine also blocked retrograde transduction of hippocampal neurons after rAAV-5 delivery to the MFB (data not shown).

Long-term EGFP expression in the STR and the SN. To investigate long-term gene expression mediated by rAAV-5, two animals were injected with rAAV-5–EGFP in the right STR and assessed 9 months later. EGFP expression remained stable from day 28 (Fig. 1) up to 9 months (Fig. 7) within the STR and the SN. Many EGFP-positive cells were readily detected within the STR, and some EGFP-positive cell bodies were found within the cortex (Fig. 7A and B). Strongly EGFP-positive fibers covered the entire ML extension of the SNr (Fig. 7C and D), and EGFP-positive cell bodies were detected within the SNc (Fig. 7C).

DISCUSSION

The nigral dopaminergic cells are the neurons that progressively degenerate in PD. Although gene transfer at the level of the SN may protect dopaminergic cell bodies from degeneration, attenuation or prevention of motor deficits will (most likely) require preservation of the dopaminergic striatal innervation as well (22, 23, 44). To preserve dopaminergic axons, it may be necessary to express "therapeutic" genes in large areas of the STR. Combined expression of genes in dopaminergic neurons and striatal cells may be necessary to provide the best benefit. This may be achieved by the simultaneous transduction of nigral dopaminergic neurons with a virus expressing an antiapoptotic gene (33) and infection of striatal tissue with a vector encoding a neurotrophic factor supporting the survival of dopaminergic axon terminals (23, 28). While widespread transduction would be desired in the STR in this setting (to reach as many axon terminals as possible), locally restricted infection of dopaminergic neurons in the SN may be preferred so as to limit the effects of the transgene to these cells. In addition, a vector with the ability for retrograde transduction is expected to facilitate surgical interventions, because it could be delivered into the STR and circumvent direct injections into the SN (which is located close to the brain stem and several other vital brain areas).

With these ideas in mind, we set out and compared the abilities of rAAV-2 and rAAV-5 vectors (with ITRs and capsid

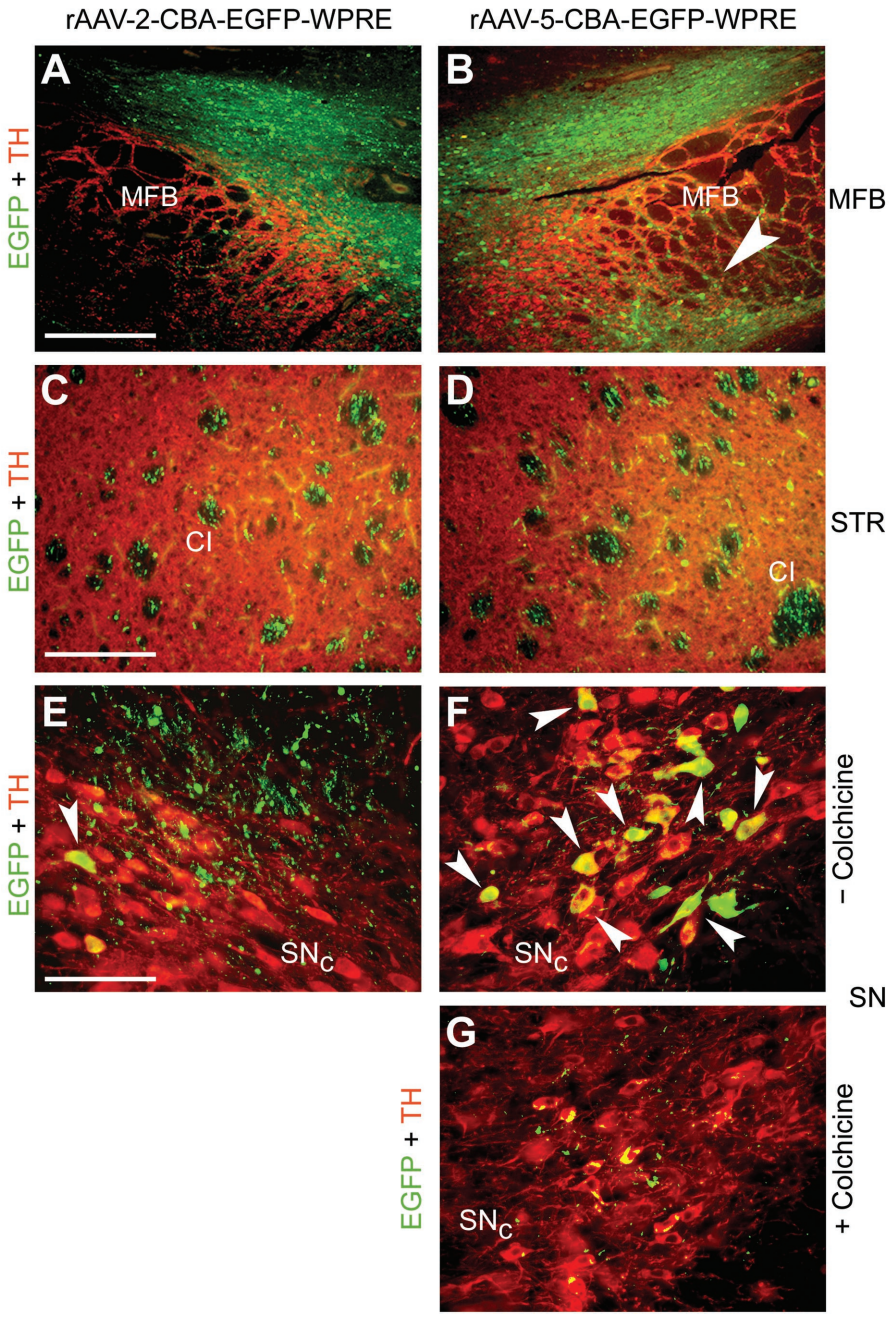

FIG. 5. EGFP expression in the MFB, the STR, and the SN after injection of rAAV-2 and rAAV-5 into the MFB. Coronal sections of the MFB, the STR, and the SN were analyzed for EGFP (green) and TH (red) expression. Representative two-color (merged) images from two animals are shown. (A and B) EGFP-positive fibers and cells were present above and within the TH-positive area of the MFB after delivery of either serotype. However, only rAAV-5 transduced cells located on the ventral part of the MFB (B, arrowhead). Bar, 250 μm. (C and D) In the STR, EGFP-positive fibers were present in the CI of both hemispheres. Bar, 125 μm. (E and F) Occasionally, EGFP-expressing dopaminergic neurons were detected in the SNc after MFB injection of rAAV-2 (E, arrowhead), while more EGFP-transduced dopaminergic neurons were present after MFB delivery of rAAV-5 (F, arrowheads). In addition, a meshwork of EGFP-positive fibers surrounding the dopaminergic neurons was observed after MFB injection with either vector serotype. (G) Colchicine injection into the MFB prior to rAAV-5 delivery almost completely blocked EGFP expression in TH-positive cell bodies within the SNc. Bar for panels E to G, 62.5 μm.

proteins derived from the same serotype) to transduce the nigrostriatal system of rats. For this purpose, the two serotypes were delivered into the SN, the STR, or the MFB. In each case, EGFP expression was investigated locally in cell bodies at the site of injection, in fibers of transduced neurons (anterograde transport of gene product) projecting to other brain areas, and in neuronal cell bodies that send axons to distantly transduced neurons (retrograde transduction). Our main findings are as follows: (i) both serotypes predominantly transduced neurons, although rAAV-5 also infected nonneuronal cells; (ii) the

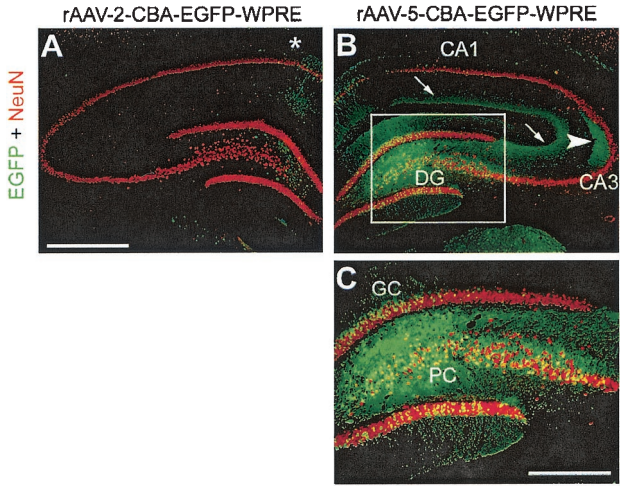

FIG. 6. EGFP expression in the hippocampus after MFB injection of rAAV-2 and rAAV-5. Coronal sections of the hippocampus were analyzed for EGFP (green) and NeuN (red) expression. Representative two-color (merged) images from one animal are shown. A few EGFP-positive fibers and cells were present along the needle tract (which passed the hippocampus during MFB injection) after rAAV-2 injection (asterisk in panel A). In contrast, rAAV-5 transduced many granule cells (GC) and pyramidal cells (PC) as well as NeuN-negative cells within the DG (B and C; panel C is a magnification of the inset in panel B). In addition, EGFP-positive mossy fibers emanating from transduced GC were detected in their target area, the CA3 region (B, arrowhead), and EGFP-positive axons of transduced PC were present in the molecular layer of the hippocampus (B, arrows). Bar for panels A and B, 500 μm. Bar for panel C, 250 μm.

rAAV-5 vector transduced significantly more cells and a much larger area in all targeted sites; (iii) transduction was spatially restricted with rAAV-2, but the level of EGFP expression was higher than with rAAV-5; and (iv) retrograde transduction was observed with rAAV-5 but not, or much less so, with rAAV-2.

Davidson and colleagues (11) first investigated rAAV-5 vectors in the rodent STR. Like us, they observed a significantly higher number of transgene (β-galactosidase)-expressing cells after injection of rAAV-5 than after rAAV-2 injection. The same authors also found that rAAV-5 transduces an appreciable number of astrocytes, while we only occasionally detected NeuN-negative (glial) cells expressing EGFP after injection of the rAAV-5 vector into the STR and the SN. This discrepancy may be explained by the fact that their rAAV-5 vector contained the Rous sarcoma virus long terminal repeat promoter, whereas both of our vectors harbored the hybrid cytomegalovirus enhancer/chicken β-actin (CBA) promoter. The most striking difference we observed between the two serotypes was that rAAV-5 transduced significantly more cells and a much broader area in all targeted brain sites. Notably, the superior transduction of neurons by rAAV-5 in the STR translated into a much denser network of EGFP-expressing fibers in the GAD-positive area of the SNr. In contrast, after striatal injection of rAAV-2, EGFP-positive fibers were confined to the medial part of the SNr. These observations are in good agreement with the lamellar relationship between the SNr and the STR (12). Locally restricted transduction (around the injection

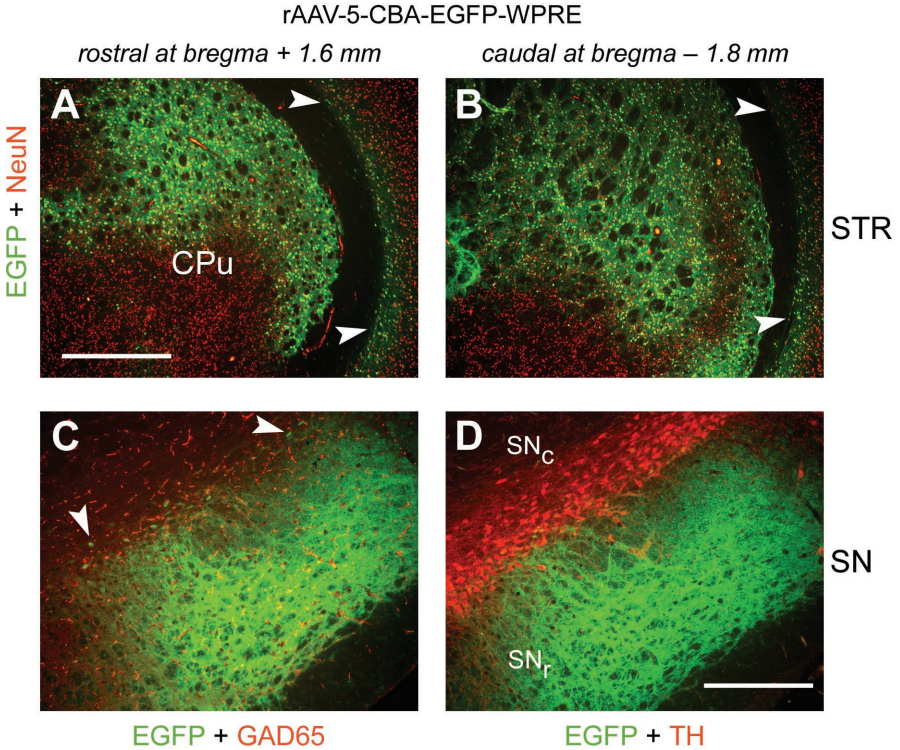

FIG. 7. EGFP expression in the STR and the SN 9 months after striatal injection of rAAV-5. Coronal sections of the STR and the SN of the right hemisphere were analyzed for expression of EGFP (green), TH (red), GAD65 (red), and NeuN (red) 9 months after rAAV-5–EGFP injections. Representative two-color (merged) images from one animal are shown. (A and B) Within the rostral and caudal parts of the STR, EGFP expression was widespread. EGFP-positive cells were also detected in the cortex (arrowheads). CPu, caudate putamen. Bar, 500 μm. (C and D) Strongly EGFP-positive fibers were present within the entire area of the SNr. EGFP-positive cell bodies were distributed over the ML extension of the SNc (C, arrowheads). Bar, 250 μm.

site) in the STR by rAAV-2 has been reported previously (50). Our results confirm these findings and the observation that the tropism of rAAV-2 is higher for neurons of the GP than for cells located in the caudate putamen (see Fig. 1). In addition to this work (50), we also find that retrograde transduction of dopaminergic neurons in the SNc can be achieved by injection of either vector into the STR, although the efficiency of retrograde transduction is considerably higher for rAAV-5. While it is known that some neurotrophic factors can be transported in a retrograde manner between cells (34), this does not apply to proteins in general. Thus, glial cell line-derived neurotrophic factor (GDNF), but not β-galactosidase, was expressed in motoneurons after delivery of rAAV vectors encoding these proteins into skeletal muscle (31). We therefore believe that EGFP expression in nigral dopaminergic cell bodies is the result of retrograde transport of the viral particles within dopaminergic axons that were infected in the STR. Indeed, evidence for retrograde transport of fluorescently labeled AAV-2 particles in the nigrostriatal system has been presented previously (21). Furthermore, we demonstrate the stability of EGFP expression in the STR and the SN after striatal delivery of rAAV-5 for as long as 9 months. To our knowledge, this is the longest period described for a nonpseudotyped rAAV-5 vector in the brain.

Interestingly, we also observed expression of EGFP in retrogradely transduced striatal neurons after nigral delivery of rAAV-5 (but not rAAV-2). Morphologically, the transduced cells resembled gamma aminobutyric acid-positive, medium-sized spiny projection neurons. Such a transduction pattern has not been reported previously, and it suggests the interesting possibility of selectively transducing striatal neurons that participate in, and are regulated by, the nigrostriatal network.

While rAAV-2 transduction was locally restricted, EGFP expression levels in individual cells and their axons were generally higher than those achieved with rAAV-5. It is likely that serotype-specific affinities for cell surface attachment and internalization receptors at least partially account for this difference. Heparan sulfate proteoglycans (49), integrins (48), and fibroblast growth factor receptor 1 (43) are important receptors for AAV-2. Heparan sulfate proteoglycans are heavily expressed at the surfaces and in the extracellular matrix of neurons, thus preventing the spread of rAAV-2 in the parenchyma and possibly mediating multiple transduction events. Recently, N-linked sialic acid (20) and platelet-derived growth factor receptor (37) were identified as receptors for AAV-5, and their expression in vivo correlates well with the observed transduction profile of rAAV-5 (37). However, we cannot be certain that the capsid-receptor interactions alone account for the differences in expression levels seen between rAAV-2 and rAAV-5, because we cannot formally exclude distinct effects of the serotype-specific ITRs on gene expression from the CBA promoter.

We did not detect EGFP expression by native fluorescence microscopy in the STR after nigral delivery of either AAV serotype. This finding was surprising, because we had previously shown that dopaminergic expression of EGFP from an rAAV-2 vector containing the neuron-specific human platelet-derived growth factor β-chain promoter could be readily detected in the STR (40). Moreover, EGFP expression in striatal dopaminergic axons had been observed by others (27) with the same CBA promoter that was used in this study, but the different outcomes may be explained by the roughly 12-fold-lower virus dose injected in our study.

Delivery of the rAAV vectors into the MFB was investigated as a possibility for the simultaneous transduction of both nigral dopaminergic neurons and striatal axons. However, transduction by both serotype vectors was largely confined to the injected MFB, and only in the case of rAAV-5 did we observe a few EGFP-positive nigral dopaminergic neurons (Fig. 5F). Colchicine injections into the MFB blocked EGFP expression in dopaminergic neurons of the SNc and the VTA after rAAV-5 delivery into the MFB (Fig. 5G). This shows that MFB injection of rAAV-5 results in the transduction of TH-positive cell bodies in the SNc and VTA by retrograde transport rather than by passive diffusion.

Transduction of hippocampal neurons after direct injection of rAAV-2 and rAAV-5 into the hippocampus has been described previously (26, 36, 37). However, to our surprise, we found that the hippocampus was also efficiently transduced in several animals after MFB injection of rAAV-5. Specifically, rAAV-5 mediated widespread transduction of granule and pyramidal cells in the DG (Fig. 6B and C). Although we cannot exclude the possibility that a small amount of virus solution may have leaked out during needle insertion or retraction, it is very unlikely that this alone would account for the widespread transduction in the hippocampus that we observed. Rather, we favor the idea that the hippocampal neurons were transduced by retrograde transport of virus particles that were taken up into axons in the MFB. Supporting this view is the observation that rAAV-5-mediated EGFP expression in hippocampal cell bodies was completely suppressed when colchicine was injected into the MFB prior to vector delivery (data not shown). Also, if hippocampal neurons were transduced by virus leakage in this structure, we would expect to find EGFP expression in fibers of the contralateral hippocampus (26), but this was not observed (see Fig. 6A). In fact, it has long been known that the MFB receives afferent innervation from the hippocampus and that lesions in the hippocampus can be generated by injection of 6-hydroxydopamine into the MFB (2). Again, the lack of hippocampal transduction after MFB injection of rAAV-2 argues that retrograde transduction by rAAV-5 is more effective. These observations are exciting in view of the important function of the hippocampus for learning and memory, and the increasing evidence of its involvement in human psychological disorders such as schizophrenia and depression (46, 47).

In summary, our results highlight the differences and specific properties of rAAV-2 and rAAV-5 vectors in the rat nigrostriatal system. Our findings should be useful for the development of improved gene therapy approaches for PD and possibly other central nervous system diseases affecting the STR and/or the hippocampus.

ACKNOWLEDGMENTS

We thank Ana Jongen, Anna Mura (both of the Laboratory of Behavioural Neurobiology, ETH Zurich), and Oliver Weinmann (Brain Research Institute, University of Zurich) for helpful discussions. We acknowledge the gift of the pCBA-GFP-WPRE plasmid from Ronald L. Klein (Louisiana State University). Plasmid pDG (from Juergen Kleinschmidt, University of Heidelberg) and plasmids pAAV5.1-EGFP, pack5.1, and pAdΔF6 (from James Wilson, University of Pennsylvania) were obtained via material transfer agreements.

This work was supported by a grant from the Swiss National Science Foundation to H.B. and from the National Center of Competence in Research for Neural Plasticity and Repair.

REFERENCES

1. **Alisky, J. M., S. M. Hughes, S. L. Sauter, D. Jolly, T. W. Dubensky, Jr., P. D. Staber, J. A. Chiorini, and B. L. Davidson.** 2000. Transduction of murine cerebellar neurons with recombinant FIV and AAV5 vectors. Neuroreport **11:**2669–2673.
2. **Arvin, B., E. Le Peillet, N. Durmuller, A. G. Chapman, and B. S. Meldrum.** 1992. Electrolytic lesions of the locus coeruleus or 6-hydroxydopamine lesions of the medial forebrain bundle protect against excitotoxic damage in rat hippocampus. Brain Res. **579:**279–284.
3. **Auricchio, A., G. Kobinger, V. Anand, M. Hildinger, E. O'Connor, A. M. Maguire, J. M. Wilson, and J. Bennett.** 2001. Exchange of surface proteins impacts on viral vector cellular specificity and transduction characteristics: the retina as a model. Hum. Mol. Genet. **10:**3075–3081.
4. **Boulis, N. M., N. E. Willmarth, D. K. Song, E. L. Feldman, and M. J. Imperiale.** 2003. Intraneural colchicine inhibition of adenoviral and adeno-associated viral vector remote spinal cord gene delivery. Neurosurgery **52:** 381–387.
5. **Chao, H., Y. Liu, J. Rabinowitz, C. Li, R. J. Samulski, and C. E. Walsh.** 2000. Several log increase in therapeutic transgene delivery by distinct adeno-associated viral serotype vectors. Mol. Ther. **2:**619–623.
6. **Chiorini, J. A., F. Kim, L. Yang, and R. M. Kotin.** 1999. Cloning and characterization of adeno-associated virus type 5. J. Virol. **73:**1309–1319.
7. **Chiorini, J. A., L. Yang, Y. Liu, B. Safer, and R. M. Kotin.** 1997. Cloning of adeno-associated virus type 4 (AAV4) and generation of recombinant AAV4 particles. J. Virol. **71:**6823–6833.
8. **Choi-Lundberg, D. L., Q. Lin, Y. N. Chang, Y. L. Chiang, C. M. Hay, H. Mohajeri, B. L. Davidson, and M. C. Bohn.** 1997. Dopaminergic neurons protected from degeneration by GDNF gene therapy. Science **275:**838–841.
9. **Costantini, L. C., D. R. Jacoby, S. Wang, C. Fraefel, X. O. Breakefield, and O. Isacson.** 1999. Gene transfer to the nigrostriatal system by hybrid herpes simplex virus/adeno-associated virus amplicon vectors. Hum. Gene Ther. **10:**2481–2494.
10. **Cucchiarini, M., X. L. Ren, G. Perides, and E. F. Terwilliger.** 2003. Selective gene expression in brain microglia mediated via adeno-associated virus type 2 and type 5 vectors. Gene Ther. **10:**657–667.
11. **Davidson, B. L., C. S. Stein, J. A. Heth, I. Martins, R. M. Kotin, T. A. Derksen, J. Zabner, A. Ghodsi, and J. A. Chiorini.** 2000. Recombinant adeno-associated virus type 2, 4, and 5 vectors: transduction of variant cell types and regions in the mammalian central nervous system. Proc. Natl. Acad. Sci. USA **97:**3428–3432.
12. **Deniau, J. M., A. Menetrey, and S. Charpier.** 1996. The lamellar organization of the rat substantia nigra pars reticulata: segregated patterns of striatal afferents and relationship to the topography of corticostriatal projections. Neuroscience **73:**761–781.
13. **During, M. J., J. R. Naegele, K. L. O'Malley, and A. I. Geller.** 1994. Long-term behavioral recovery in parkinsonian rats by an HSV vector expressing tyrosine hydroxylase. Science **266:**1399–1403.
14. **Edstrom, A., M. Hanson, M. Wallin, and B. Cederholm.** 1979. Inhibition of fast axonal transport and microtubule polymerization in vitro by colchicine and colchiceine. Acta Physiol. Scand. **107:**233–237.
15. **Frain, O., and V. Leviel.** 1998. Mesencephalic THmRNA-reduced expression by blocking axonal transport with colchicine. Neuroreport **9:**1529–1532.
16. **Gao, G. P., M. R. Alvira, L. Wang, R. Calcedo, J. Johnston, and J. M. Wilson.** 2002. Novel adeno-associated viruses from rhesus monkeys as vectors for human gene therapy. Proc. Natl. Acad. Sci. USA **99:**11854–11859.
17. **Grimm, D., A. Kern, K. Rittner, and J. A. Kleinschmidt.** 1998. Novel tools for production and purification of recombinant adenoassociated virus vectors. Hum. Gene Ther. **9:**2745–2760.
18. **Grimm, D., S. Zhou, H. Nakai, C. E. Thomas, T. A. Storm, S. Fuess, T. Matsushita, J. Allen, R. Surosky, M. Lochrie, L. Meuse, A. McClelland, P. Colosi, and M. A. Kay.** 2003. Preclinical in vivo evaluation of pseudotyped adeno-associated virus vectors for liver gene therapy. Blood **102:**2412–2419.
19. **Hardy, J., M. R. Cookson, and A. Singleton.** 2003. Genes and parkinsonism. Lancet Neurol. **2:**221–228.
20. **Kaludov, N., K. E. Brown, R. W. Walters, J. Zabner, and J. A. Chiorini.** 2001. Adeno-associated virus serotype 4 (AAV4) and AAV5 both require sialic acid binding for hemagglutination and efficient transduction but differ in sialic acid linkage specificity. J. Virol. **75:**6884–6893.
21. **Kaspar, B. K., D. Erickson, D. Schaffer, L. Hinh, F. H. Gage, and D. A. Peterson.** 2002. Targeted retrograde gene delivery for neuronal protection. Mol. Ther. **5:**50–56.
22. **Kirik, D., B. Georgievska, C. Burger, C. Winkler, N. Muzyczka, R. J. Mandel, and A. Bjorklund.** 2002. Reversal of motor impairments in parkinsonian rats by continuous intrastriatal delivery of L-dopa using rAAV-mediated gene transfer. Proc. Natl. Acad. Sci. USA **99:**4708–4713.
23. **Kirik, D., C. Rosenblad, A. Bjorklund, and R. J. Mandel.** 2000. Long-term rAAV-mediated gene transfer of GDNF in the rat Parkinson's model: intrastriatal but not intranigral transduction promotes functional regeneration in the lesioned nigrostriatal system. J. Neurosci. **20:**4686–4700.
24. **Kitada, T., S. Asakawa, N. Hattori, H. Matsumine, Y. Yamamura, S. Minoshima, M. Yokochi, Y. Mizuno, and N. Shimizu.** 1998. Mutations in the parkin gene cause autosomal recessive juvenile parkinsonism. Nature **392:** 605–608.
25. **Klein, R. L., M. E. Hamby, Y. Gong, A. C. Hirko, S. Wang, J. A. Hughes, M. A. King, and E. M. Meyer.** 2002. Dose and promoter effects of adeno-associated viral vector for green fluorescent protein expression in the rat brain. Exp. Neurol. **176:**66–74.
26. **Klein, R. L., M. E. Hamby, C. F. Sonntag, W. J. Millard, M. A. King, and E. M. Meyer.** 2002. Measurements of vector-derived neurotrophic factor and green fluorescent protein levels in the brain. Methods **28:**286–292.
27. **Klein, R. L., M. A. King, M. E. Hamby, and E. M. Meyer.** 2002. Dopaminergic cell loss induced by human A30P alpha-synuclein gene transfer to the rat substantia nigra. Hum. Gene Ther. **13:**605–612.
28. **Kordower, J. H., M. E. Emborg, J. Bloch, S. Y. Ma, Y. Chu, L. Leventhal, J. McBride, E. Y. Chen, S. Palfi, B. Z. Roitberg, W. D. Brown, J. E. Holden, R. Pyzalski, M. D. Taylor, P. Carvey, Z. Ling, D. Trono, P. Hantraye, N. Deglon, and P. Aebischer.** 2000. Neurodegeneration prevented by lentiviral vector delivery of GDNF in primate models of Parkinson's disease. Science **290:** 767–773.
29. **Kruger, R., W. Kuhn, T. Muller, D. Woitalla, M. Graeber, S. Kosel, H. Przuntek, J. T. Epplen, L. Schols, and O. Riess.** 1998. Ala30Pro mutation in the gene encoding alpha-synuclein in Parkinson's disease. Nat. Genet. **18:** 106–108.
30. **Leroy, E., R. Boyer, G. Auburger, B. Leube, G. Ulm, E. Mezey, G. Harta, M. J. Brownstein, S. Jonnalagada, T. Chernova, A. Dehejia, C. Lavedan, T. Gasser, P. J. Steinbach, K. D. Wilkinson, and M. H. Polymeropoulos.** 1998. The ubiquitin pathway in Parkinson's disease. Nature **395:**451–452.
31. **Lu, Y. Y., L. J. Wang, S. Muramatsu, K. Ikeguchi, K. Fujimoto, T. Okada, H. Mizukami, T. Matsushita, Y. Hanazono, A. Kume, T. Nagatsu, K. Ozawa, and I. Nakano.** 2003. Intramuscular injection of AAV-GDNF results in sustained expression of transgenic GDNF, and its delivery to spinal motoneurons by retrograde transport. Neurosci. Res. **45:**33–40.
32. **Mastakov, M. Y., K. Baer, R. M. Kotin, and M. J. During.** 2002. Recombinant adeno-associated virus serotypes 2- and 5-mediated gene transfer in the mammalian brain: quantitative analysis of heparin co-infusion. Mol. Ther. **5:**371–380.
33. **Mochizuki, H., H. Hayakawa, M. Migita, M. Shibata, R. Tanaka, A. Suzuki, Y. Shimo-Nakanishi, T. Urabe, M. Yamada, K. Tamayose, T. Shimada, M. Miura, and Y. Mizuno.** 2001. An AAV-derived Apaf-1 dominant negative inhibitor prevents MPTP toxicity as antiapoptotic gene therapy for Parkinson's disease. Proc. Natl. Acad. Sci. USA **98:**10918–10923.
34. **Neet, K. E., and R. B. Campenot.** 2001. Receptor binding, internalization, and retrograde transport of neurotrophic factors. Cell. Mol. Life Sci. **58:** 1021–1035.
35. **Nomoto, T., T. Okada, K. Shimazaki, H. Mizukami, T. Matsushita, Y. Hanazono, A. Kume, K. Katsura, Y. Katayama, and K. Ozawa.** 2003. Distinct patterns of gene transfer to gerbil hippocampus with recombinant adeno-associated virus type 2 and 5. Neurosci. Lett. **340:**153–157.
36. **Okada, T., T. Nomoto, K. Shimazaki, W. Lijun, Y. Lu, T. Matsushita, H. Mizukami, M. Urabe, Y. Hanazono, A. Kume, S. Muramatsu, I. Nakano, and K. Ozawa.** 2002. Adeno-associated virus vectors for gene transfer to the brain. Methods **28:**237–247.
37. **Pasquale, G. D., B. L. Davidson, C. S. Stein, I. Martins, D. Scudiero, A. Monks, and J. A. Chiorini.** 2003. Identification of PDGFR as a receptor for AAV-5 transduction. Nat. Med. **9:**1306–1312.
38. **Passini, M. A., D. J. Watson, C. H. Vite, D. J. Landsburg, A. L. Feigenbaum, and J. H. Wolfe.** 2003. Intraventricular brain injection of adeno-associated virus type 1 (AAV1) in neonatal mice results in complementary patterns of neuronal transduction to AAV2 and total long-term correction of storage lesions in the brains of beta-glucuronidase-deficient mice. J. Virol. **77:**7034–7040.
39. **Paterna, J. C., and H. Bueler.** 2002. Recombinant adeno-associated virus vector design and gene expression in the mammalian brain. Methods **28:** 208–218.
40. **Paterna, J. C., T. Moccetti, A. Mura, J. Feldon, and H. Bueler.** 2000. Influence of promoter and WHV post-transcriptional regulatory element on AAV-mediated transgene expression in the rat brain. Gene Ther. **7:**1304–1311.
41. **Paxinos, G., and C. Watson.** 1986. The rat brain in sterotaxic coordinates, 2nd ed. Academic Press, New York, N.Y.
42. **Polymeropoulos, M. H., C. Lavedan, E. Leroy, S. E. Ide, A. Dehejia, A. Dutra, B. Pike, H. Root, J. Rubenstein, R. Boyer, E. S. Stenroos, S. Chandrasekharappa, A. Athanassiadou, T. Papapetropoulos, W. G. Johnson, A. M. Lazzarini, R. C. Duvoisin, G. Di Iorio, L. I. Golbe, and R. L. Nussbaum.** 1997. Mutation in the alpha-synuclein gene identified in families with Parkinson's disease. Science **276:**2045–2047.
43. **Qing, K., C. Mah, J. Hansen, S. Zhou, V. Dwarki, and A. Srivastava.** 1999. Human fibroblast growth factor receptor 1 is a co-receptor for infection by adeno-associated virus 2. Nat. Med. **5:**71–77.

44. **Rosenblad, C., D. Kirik, and A. Bjorklund.** 2000. Sequential administration of GDNF into the substantia nigra and striatum promotes dopamine neuron survival and axonal sprouting but not striatal reinnervation or functional recovery in the partial 6-OHDA lesion model. Exp. Neurol. **161:**503–516.
45. **Rutledge, E. A., C. L. Halbert, and D. W. Russell.** 1998. Infectious clones and vectors derived from adeno-associated virus (AAV) serotypes other than AAV type 2. J. Virol. **72:**309–319.
46. **Santarelli, L., M. Saxe, C. Gross, A. Surget, F. Battaglia, S. Dulawa, N. Weisstaub, J. Lee, R. Duman, O. Arancio, C. Belzung, and R. Hen.** 2003. Requirement of hippocampal neurogenesis for the behavioral effects of antidepressants. Science **301:**805–809.
47. **Schmajuk, N. A.** 2001. Hippocampal dysfunction in schizophrenia. Hippocampus **11:**599–613.
48. **Summerford, C., J. S. Bartlett, and R. J. Samulski.** 1999. αvβ5 integrin: a co-receptor for adeno-associated virus type 2 infection. Nat. Med. **5:**78–82.
49. **Summerford, C., and R. J. Samulski.** 1998. Membrane-associated heparan sulfate proteoglycan is a receptor for adeno-associated virus type 2 virions. J. Virol. **72:**1438–1445.
50. **Tenenbaum, L., F. Jurysta, A. Stathopoulos, Z. Puschban, C. Melas, W. T. Hermens, J. Verhaagen, B. Pichon, T. Velu, and M. Levivier.** 2000. Tropism of AAV-2 vectors for neurons of the globus pallidus. Neuroreport **11:**2277–2283.
51. **Wang, C., C. M. Wang, K. R. Clark, and T. J. Sferra.** 2003. Recombinant AAV serotype 1 transduction efficiency and tropism in the murine brain. Gene Ther. **10:**1528–1534.
52. **Xiao, W., N. Chirmule, S. C. Berta, B. McCullough, G. Gao, and J. M. Wilson.** 1999. Gene therapy vectors based on adeno-associated virus type 1. J. Virol. **73:**3994–4003.
53. **Zabner, J., M. Seiler, R. Walters, R. M. Kotin, W. Fulgeras, B. L. Davidson, and J. A. Chiorini.** 2000. Adeno-associated virus type 5 (AAV5) but not AAV2 binds to the apical surfaces of airway epithelia and facilitates gene transfer. J. Virol. **74:**3852–3858.
54. **Zhang, Y., N. Chirmule, G. Gao, and J. Wilson.** 2000. CD40 ligand-dependent activation of cytotoxic T lymphocytes by adeno-associated virus vectors in vivo: role of immature dendritic cells. J. Virol. **74:**8003–8010.
55. **Zolotukhin, S., B. J. Byrne, E. Mason, I. Zolotukhin, M. Potter, K. Chesnut, C. Summerford, R. J. Samulski, and N. Muzyczka.** 1999. Recombinant adeno-associated virus purification using novel methods improves infectious titer and yield. Gene Ther. **6:**973–985.